A Novel Type V TA System Where mRNA for Toxin GhoT is Cleaved by Antitoxin GhoS

Xiaoxue Wang[1,2,†], **Dana M. Lord**[5,†], **Hsin-Yao Cheng**[4,†], **Devon O. Osbourne**[4], **Seok Hoon Hong**[2], **Viviana Sanchez-Torres**[2], **Cecilia Quiroga**[4], **Kevin Zheng**[6], **Torsten Herrmann**[7], **Wolfgang Peti**[5], **Michael J. Benedik**[3], **Rebecca Page**[6,*], and **Thomas K. Wood**[2,3,4,*]

[1]Key Laboratory of Marine Bio-Resources Sustainable Utilization, South China Sea Institute of Oceanology, Chinese Academy of Sciences, Guangzhou, 510301, P. R. China

[2]Department of Chemical Engineering, Texas A & M University, College Station, Texas 77843-3122, USA

[3]Department of Biology, Texas A & M University, College Station, Texas 77843-3122, USA

[4]Departments of Chemical Engineering and Biochemistry and Molecular Biology, Pennsylvania State University, University Park, Pennsylvania 16802-4400, USA

[5]Department of Molecular Pharmacology, Physiology, and Biotechnology, Brown University, Providence, Rhode Island 02912

[6]Department of Molecular Biology, Cell Biology and Biochemistry, Brown University, Providence, Rhode Island 02912

[7]Centre Européen de RMN à très Hauts Champs, Université de Lyon/CNRS/ENS, Lyon, France 69100

SUMMARY

Among bacterial toxin/antitoxin (TA) systems, to date no antitoxin has been identified that functions by cleaving toxin mRNA. Here we demonstrate YjdO (renamed GhoT) is a membrane lytic peptide that causes ghost cell formation (lysed cells with damaged membranes) and increases persistence (persister cells are tolerant to antibiotics without undergoing genetic change). GhoT is part of a novel TA system with YjdK (renamed GhoS) since *in vitro* RNA degradation studies, qRT-PCR, and whole-transcriptome studies revealed GhoS masks GhoT toxicity by cleaving specifically *ghoT* mRNA. Alanine substitutions showed arginine 28 is important for GhoS activity, and RNA sequencing indicated the GhoS cleavage site is rich in uridine and adenosine.

*To whom correspondence should be addressed: TWood@engr.psu.edu; Rebecca_Page@brown.edu.
†These authors contributed equally to this work.

The NMR structure of GhoS indicates it is related to the CAS2 CRISPR RNase, and GhoS is a monomer. Hence, GhoT/GhoS is the first type V TA system where a protein antitoxin inhibits the toxin by cleaving specifically its mRNA.

Keywords

Toxin/antitoxin; Persistence; GhoT/GhoS

INTRODUCTION

Toxin/antitoxin (TA) systems are found in nearly all bacterial chromosomes[1] which attests to their importance in cell physiology. TA systems have been classified as type I if the antitoxin RNA prevents the translation of toxin RNA, type II if the antitoxin protein binds and inhibits the toxin protein, and type III if the antitoxin RNA binds and inhibits the protein toxin[2]. Also, a type IV designation has been proposed recently for a TA system in which the protein antitoxin interferes with binding of the toxin to its target rather than by inhibiting the toxin via direct antitoxin/toxin binding[3]. Toxins inhibit growth (e.g., inhibit translation via mRNA degradation), and antitoxins reduce toxin activity; however, antitoxins are generally labile under various stress conditions, which results in toxin activation[2].

The role of TA systems in cell physiology, specifically in biofilm formation[4, 5], persister cell formation[6, 7], and the general stress response[8, 9] is becoming more clear. Notably, mRNA endoribonuclease toxins are becoming recognized as global regulators that alter gene regulation by cleaving specific mRNAs (termed differential mRNA decay)[10]. For example, upon antibiotic stress, toxin MazF degrades most mRNAs with ACA sequences. However, its activity also results in the preferential synthesis of a subset of small proteins whose mRNAs are not degraded[11]. Since these enriched proteins are necessary both for toxicity and for survival[11], MazF acts as a regulatory factor[12].

The toxin MqsR (<u>m</u>otility <u>q</u>uorum <u>s</u>ensing <u>r</u>egulator, YgiU/B3022)[4, 13] is also a global regulator[13, 14] and is conserved in 40 eubacteria[13]. Its specific mRNA endoribonuclease activity leads to enrichment of mRNAs that code for the stress-associated proteins CstA, CspD, RpoS, Dps, and HokD[14]. In addition, 14 *Escherichia coli* mRNA transcripts do not contain the MqsR-preferred GCU cleavage site[15, 16], and six of these (*pheL, tnaC, trpL, yciG, ygaQ* and *ralR*) are differentially regulated in biofilms[17]. Another one of these 14 transcripts that lacks GCU sites is *yjdO* (B4559, renamed here as *ghoT* for toxin producing <u>gh</u>ost cells); its protein is conserved in *E. coli* and *Shigella* sp. and has not been previously characterized.

As an indicator of its impact on cell physiology through differential mRNA decay, MqsR is the first toxin that, upon inactivation, decreases the formation of persister cells[6]. Persister cells are a small fraction of bacteria that exhibit tolerance to antibiotics without genetic change[18]; it is believed they survive antibiotic treatment by becoming metabolically dormant[19]. The crucial regulator of MqsR toxicity, antitoxin MqsA (YgiT/B3021)[20], is the first antitoxin shown to be a global regulator, as transcription of loci such as *rpoS* are

derepressed upon MqsA degradation during oxidative stress[9, 14], which play critical roles in bacterial cell physiology during stress.

It is well established that endoribonuclease toxins, including MqsR[6] and RelE[21], and the kinase HipA[21, 22] inhibit protein synthesis, which is correlated with the formation of persister cells and, in turn, an increase in multi-drug tolerance. Moreover, isolated persister cells also show increased transcription of the toxin genes *mqsR*[23], *relE*[21], and *mazF*[21]. The mechanism(s) underlying the increased persistence observed upon expression of these toxins, however, has not been fully characterized. Here we present evidence that the product of one of the transcripts that lacks the primary MqsR GCU site, GhoT, increases persistence and that GhoT/GhoS (YjdO/YjdK) is a novel TA system. We show that toxin GhoT, when produced, leads to both cell death or, in the absence of cell death, an increase in persister cells. Moreover, GhoT/GhoS is the first non-type I chromosomal TA system that encodes a presumed membrane-lytic protein.

Unexpectedly and most interestingly, the antitoxin GhoS does not function like a typical antitoxin, as it is not labile during stress and it does not bind DNA to regulate transcription. Because its sequence does not resemble any protein whose structure or function was known, we used biomolecular NMR spectroscopy to determine its three dimensional structure. GhoS adopts a ferredoxin-like fold that is most similar to CRISPR-associated-2 (CAS2) sequence-specific endoribonucleases. We show that GhoS is a sequence-specific endoribonuclease that cleaves *ghoT* mRNA, preventing its translation. Thus, GhoT/GhoS is the first example of a TA system where the antitoxin protein cleaves the toxin mRNA; we classify this as a type V TA system.

RESULTS

GhoT increases persistence

Initially, we examined the 14 *E. coli* transcripts that lack GCU sites to determine if these transcripts were related to the ability of MqsR to increase persistence[6]. The effect of producing MqsR from pCA24N-*mqsR* in each of the 14 isogenic single gene knockouts (*ghoT, hisL, kilR, pheL, ralR, tnaC, trpL, yahH, ybfQ, ybhT, yciG, ygaQ, yheV,* and *ymdF*) (see Supplementary Results, Supplementary Table 1) was investigated 2 h after the addition of ampicillin (100 μg/mL) to determine if the ability of MqsR to increase persistence was altered and found that deleting *ghoT* had one of the largest effects on MqsR-mediated persistence (Supplementary Table 2). In strains where the kanamycin gene replacement might create a polar effect, the resistance gene was removed and the strains retested. In no case could the effects be ascribed to polarity (Supplementary Table 2). A time course study further confirmed that deleting *ghoT* significantly reduced MqsR-mediated persistence (27 ± 2-fold reduction for *ghoT*/pCA24N-*mqsR* vs. BW25113/pCA24N-*mqsR*) and made the cell behave similarly to the wild-type strain without MqsR production (Fig. 1a). Corroborating the dependence of MqsR on GhoT to increase persistence, producing GhoT in a *ghoT* strain also increased persistence 48 ± 3 fold to levels seen while producing MqsR (Fig. 1b). In fresh LB medium, some of these persister cells revived with a lag time of roughly 4 h which is comparable to reported values[24] (Fig. 1c).

GhoT affects the membrane and produces ghost cells

The organization of the *ghoST* operon and the impact of GhoT on persistence suggested that it might be a TA pair (Supplementary Fig. 1a). Hence, we tested whether or not GhoT is a toxin. GhoT is predicted to be a small (57 aa), highly hydrophobic protein with two transmembrane domains (residues 7 to 27 and 37 to 57)[25]. When GhoT was produced in the wild-type strain, which contains a chromosomal gene for the putative antitoxin GhoS, the turbidity of the culture decreased (Fig. 2a), and this decrease was due to cell lysis since cell cultures became clear (Fig. 2b). Corroborating these results, production of GhoT caused 60% of the cells to adopt "ghost" morphologies as observed using phase contrast microscopy (Fig. 2c); ghost cells are dead or dying cells in which the damaged membrane causes the cell poles to appear dense and the center to appear transparent[26]. Therefore, GhoT is a toxin that when overproduced, lyses cells by disrupting the cell membrane to form ghost cells.

GhoS is an antitoxin and GhoT/GhoS form a TA pair

Like toxin GhoT, GhoS is also a small protein (98 aa). There are 27 bp between the two genes, which include a putative RBS for *ghoT*; therefore, *ghoST* are predicted to comprise a single operon. Unlike GhoT, production of GhoS was not toxic, and it completely counteracted the toxicity of GhoT (Fig. 2a). Furthermore, production of GhoS with GhoT reduced the formation of ghost cells by 18-fold based on microscopic observation of ~ 500 cells (Fig. 2c), whereas producing GhoS alone did not cause ghost cells to form.

Replacement of antitoxin *ghoS* with a kanamycin cassette[27] is not lethal, likely due to the polar effect on downstream *ghoT*. However, when GhoT was produced via pCA24N-*ghoT*, deletion of *ghoS* was lethal as growth was completely inhibited in the *ghoS* mutant but not in the *ghoT* mutant, which has an intact chromosomal copy of *ghoS* (Fig. 2d). This is a typical feature of TA systems[20], although polar mutations can mask this effect if the antitoxin gene precedes the toxin gene.

As shown by reverse transcription polymerase chain reaction (RT-PCR), *ghoST* form a single operon since they are co-transcribed. Specifically, a single band of ~400 bp was detected using a forward primer in the first gene (*ghoS*-f) and a reverse primer in the second gene (*ghoT*-r) (Supplementary Table 3) using cDNA synthesized from total RNA as the template (Supplementary Fig. 1b). As controls, the same band was detected using genomic DNA as template but not for total RNA. Collectively, these results demonstrate that GhoS is an antitoxin, that *ghoT* and *ghoS* are co-transcribed, and that they form a TA system.

GhoS is a proteic monomeric antitoxin

To demonstrate that GhoS functions as a proteic antitoxin, we introduced a stop codon by a single nucleotide change into *ghoS* DNA at corresponding amino acid position 16 (Tyr16) and tested its impact on cell growth. We found that the early termination mutation abolished the ability of GhoS to block the toxicity of GhoT for both cell growth (Fig. 2a) and ghost cell formation. We also found that antitoxin GhoS is not degraded (Supplementary Fig. 2a) in response to stress[28], whereas most antitoxins are degraded (Supplementary Fig. 2b), and found that GhoS does not bind its own promoter (Supplementary Fig. 3). In addition, size

exclusion chromatography, dynamic light scattering (Supplementary Fig. 4) and biomolecular NMR experiments (see below) demonstrated that GhoS is a monomer in solution. Collectively, these results show that GhoS is a non-canonical antitoxin because it does not regulate its own transcription, it is stable, and it is a monomer in solution.

GhoS adopts a ferredoxin-like fold similar to CAS2

Analysis of the GhoS protein sequence using BLAST revealed that while it is conserved among multiple species of *E. coli*, it is not similar to any protein whose structure or function is known. Because function is more highly conserved than sequence, we used biomolecular NMR spectroscopy to determine the structure of GhoS and, in turn, gain insights into its biological function. In the sequence-specific backbone assignment, 95 of the expected 96 backbone amide NH pairs (3 prolines) are assigned with the missing residue corresponding to the N-terminal cloning artifact His(−1) (Supplementary Fig. 5). A total of 2479 Nuclear Overhauser Enhancement (NOE)-derived distance constraints were used for the structure calculation (~25 NOE constraints/residue) using a simulated annealing protocol within the program CYANA[29–31] and refined in explicit solvent using CNS[32]. The GhoS model has excellent stereochemistry (see Supplementary Methods) and the root-mean-square-deviation value about the mean coordinate positions of the backbone atoms for residues 5 to 95 is 0.36 ± 0.08 Å (20 models in the ensemble; Supplementary Fig. 6a). NMR and refinement statistics are reported in Supplementary Table 4. The three-dimensional GhoS structure consists of three α-helices and five β-strands (Fig. 3a) and is stabilized by two hydrophobic clusters. The central hydrophobic core consists of residues Tyr10, Val12, Phe14, Tyr16, Phe24, Leu27, Met31, Met34, Phe36, Phe55, Ile57, Ile66, Ile70, Leu77, Ile80, Phe82, Leu84, and Ile86 (Supplementary Fig. 6b). The structure is also stabilized by a second hydrophobic cluster comprised of Val11, Val40, Leu50, Ala56, Met87, Val89, Tyr92, and Phe93 (Supplementary Fig. 6c).

A search for structural homologs of GhoS using the structure-based alignment program DALI[33] identified five proteins with Z-scores of 5.8 to 6.3, all of which adopt a ferredoxin-like fold, characterized by a split α-β sandwich (β-α-β-β-α-β; Supplementary Table 5). This superfold is highly populated with functionally diverse proteins, such as ribosomal proteins, DNA binding proteins, and ribonucleases[34]. Of the five structures with the best Z-scores, only two were of similar size to GhoS: SSO1404 (PDBID 2I8E, 88 residues; Z-score = 6.1)[35] and SSO8090 (PDBID 3EXC, 78 residues; Z-score = 5.8). These proteins (and three other family members: TT1823, Z-score = 5.6, PF1117, Z-score=5.1, DvuCAS2, Z-score = 5.0[36]) belong to the CRISPR-associated (CAS2) family. SSO1404 and SSO8090 are sequence-specific endoribonucleases that preferentially cleave single-stranded RNA[37]. The structures of GhoS and the CAS2 protein SSO1404 monomer (CAS2 proteins are dimers *in vitro*) overlap well (Supplementary Fig. 6d,e, Supplementary Fig. 7). The primary difference between them is the position of β-strand β2. In GhoS, β2 and β2' form a short two-stranded β-sheet that interacts with the C-terminal α-helix, α3. In contrast, in the CAS2 proteins, β2 projects upwards to form the fourth β-strand of the β-sheet in the ferredoxin fold. Thus, GhoS adopts an atypical ferredoxin fold in which the central β-sheet is made up of three and not four β-strands.

GhoS is an endoribonuclease that cleaves *ghoT* mRNA

The sequence identity between GhoS and the CAS2 proteins is low, between 10–19%. However, when the structures of SSO1404 and GhoS are superimposed, five of the six SSO1404 catalytic residues are structurally conserved in GhoS (Fig. 3a, Supplementary Fig. 6d,e; GhoS/SSO1404: Phe14/Tyr9, Asp15/Asp10, Arg26/Arg19, Arg28/Arg31 and Phe55/Phe37). Systematically converting these five GhoS residues to alanines revealed that, *in vitro*, the Arg28Ala, Phe55Ala and, to a lesser extent, Arg26Ala substitutions reduced the ability of antitoxin GhoS to cleave *ghoT* mRNA (Fig. 3b, Supplementary Fig. 8; circular dichroism shows all mutants are folded, Fig. 3c); this effect was also corroborated for the Arg28Ala variant *in vivo* (Fig. 3d). Thus Arg28 appears to be important for GhoS activity.

Because GhoS production is not toxic but instead increases growth (Fig. 2a), these results suggest that GhoS is a sequence-specific endoribonuclease. Thus, we investigated whether GhoS cleaves *ghoT* mRNA. Using quantitative real-time, reverse-transcription PCR (qRT-PCR), we found that the *ghoT* portion of the *ghoST* transcript in the wild-type strain was 21 ± 2-fold less stable than the *ghoS* portion of the transcript in the stationary phase (see Supplementary Table 6 for all of the qRT-PCR data). Corroborating this result, production of GhoS via pCA24N-*ghoS* reduced the *ghoT* portion of the transcript 5 ± 1-fold relative to the empty plasmid. Cleavage by GhoS appears specific since *ompA* (−1.1 ± 0.2), *ompF* (1.2 ± 0.1), *ralR* (−1.7 ± 0.4), or *purA* (−1.9 ± 0.5) transcript levels were not affected by GhoS production.

In vitro, GhoS cleaved the *ghoT* portion of the transcript (207 nt, Supplementary Table 7) at multiple sites and generated, after full-digestion, fragments of approximately 52, 65, 87, 91 and 116 nt (Fig. 4a & Supplementary Fig. 8), whereas there was less degradation of the *ghoS* portion of the transcript under the same conditions. As expected, heat denaturation of GhoS abolished the ability to cleave the transcripts. Very little degradation of the ATP synthase subunit gene *atpE* and *ompA in vitro* was observed. Finally, no degradation was observed of: (i) total RNAs *in vitro*, (ii) 23S and 16S rRNAs *in vivo* with GhoS, and (iii) tRNAs *in vitro* (Supplementary Fig. 9).

Using RNA sequencing, we found that GhoS cleaves specifically *ghoT* mRNA at nt positions 30/31, 51/52, 66/68, 115/116, and 154/155 (positions S1 to S5, Fig. 4b). Analysis of the cleaved products identified a putative cleavage site corresponding to 5'-UNNU(A/C)N(A/G)(A/U)A(A/U)-3'. To corroborate GhoS cleavage at the 51/52 nt site, we altered the *ghoT* mRNA fragment via mutation m1 (AUAUU to CGCGC at nt position 52–56, Fig. 4b) and found a reduction in overall cleavage and increase in larger fragments (e.g., 87 and 124 nt) as would be expected for loss of this site (Fig. 4c). Additional mutations (m2 at nt 125–128 and m3 at nt 59–64) reduced cleavage as expected given their proximity to cleavage sites 66/68 and 115/116, and the m4 change (nt 132–137) had little effect since the transcript was completely degraded as with the wild-type *ghoT* mRNA (Fig. 4c).

To investigate the importance of RNA secondary structure on GhoS cleavage, the stems disrupted by mutations m1 or m2 were recovered by the introduction of both mutations into the plasmid carrying single mutant *ghoT* alleles. The recovery of the cleavage pattern to that of the wild-type *ghoT* transcript in the double mutant transcript would indicate the

importance of RNA secondary structure over sequence recognition in GhoS cleavage, while a reduction in cleavage would indicate that sequence recognition is important. We found that the introduction of both mutations m1m2 to restore the stem of the predicted secondary structure (Fig. 4d) generated a unique cleavage pattern distinct from that of the native *ghoT* mRNA (Fig. 4e). A reduction of the fragments accumulated due to the m1 mutation along with an increase in large partially-cleaved or un-cleaved fragments compared to the native transcript suggests the importance of sequence recognition during GhoS cleavage. Therefore, GhoS is a specific RNase that limits translation of toxin GhoT by cleaving *ghoT* transcripts.

To provide more evidence of the specificity of the RNase activity of GhoS, we analyzed changes in mRNA levels during production of GhoS compared to the strain with an empty plasmid with a DNA microarray so that we could investigate *in vivo* which of the cell's transcripts may be cleaved by GhoS. Under these conditions, only 20 transcripts had altered mRNA levels and all were found to be reduced (Supplementary Table 9); there were no induced genes. These genes down-regulated due to GhoS production were all involved in the biosynthesis/transport of purines and pyrimidines. These results suggest that GhoS selectively cleaves only a few cellular targets.

To further corroborate the findings in the DNA microarray, qRT-PCR was performed with seven genes (*purM, purH, purE, pyrI, pyrB, carA* and *carB*) with total RNA isolated under the same culture conditions as the DNA microarray experiment. In each case, the qRT-PCR results showed a decreased RNA abundance upon GhoS production, which matched the microarray results (Supplementary Table 9). Although *ghoT* expression was unaltered in the microarray analysis, qRT-PCR performed with duplicate samples on three independent occasions, showed that *ghoT* expression was decreased at least 3-fold upon production of GhoS.

GhoT increases early biofilm formation

Since TA systems affect biofilm formation[4, 5] and since we identified *mqsR* as one of the highly regulated genes in *E. coli* biofilm cells, when compared to planktonic cells[4], we investigated the impact of GhoT/GhoS on biofilm formation. Deletion of *ghoT* decreased biofilm formation at 8 h in LB medium at 30°C (4.6-fold) and 37°C (4.9-fold), while deletion of *ghoS* increased biofilm formation significantly (up to 6.1-fold) at 30°C and 37°C at 8 h (Supplementary Fig. 10a). Swimming motility was also slightly reduced when *ghoT* was deleted, while the deletion of *ghoS* increased cell motility ~2-fold (Supplementary Fig. 10b). These results show that GhoS and GhoT impact early biofilm formation and swimming motility.

DISCUSSION

Collectively, our results strongly support that GhoT/GhoS form a novel type V TA pair. These results are: (i) both proteins are small, (ii) the genes form an operon (*ghoST*) since they are co-transcribed and there are only 27 bp between the coding regions of the two genes, (iii) GhoT functions as a presumed membrane toxin that not only stops growth but also, in high concentrations, lyses cells, (iv) GhoS blocks GhoT-mediated toxicity by

specifically cleaving *ghoT* transcripts at 5'-UNNU(A/C)N(A/G)(A/U)A(A/U)-3' sites and preventing its translation, and (v) deletion of antitoxin GhoS in the presence of GhoT is lethal. As a novel TA system, GhoT is the first chromosomal membrane-damaging protein to be neutralized by a protein antitoxin (cf., toxin TisB damages membranes as a type I TA system[38]). GhoS is also the first antitoxin to inhibit a toxin by cleaving its mRNA; hence, it creates a new paradigm for TA systems (we propose the type V designation). Furthermore, the GhoT/GhoS TA system is unique in that antitoxin GhoS is not proteolytically degraded during stress, and GhoS is unusual in that it does not bind its putative promoter region. For comparison, the antitoxin of the ζ–ε TA system from plasmid pSM19035 also plays no role in transcriptional control, but instead, the TA operon is repressed by a global regulator ω encoded by a gene within the same operon[39]; however, no such regulator for GhoT/GhoS has been identified. Also, the genomic *mazEF* operon of *Staphylococcus aureus* is not autoregulated by the antitoxin, but instead by an alternative sigma factor encoded by a gene downstream of the *mazEF* operon[40]. These examples illustrate the diversity of TA systems in terms of function and regulation.

Our central model for the genetic basis of persister cell formation is that TA pairs play a primary role since toxin activity induces a state of dormancy[41, 42]. This, in turn, allows cells to escape the effects of antibiotics. Here we identify a novel toxin, GhoT, that increases persistence by damaging the cell membrane. The precise mechanism by which GhoT leads to the loss of membrane integrity while rendering the cells dormant (viable) in the presence of ampicillin is currently unclear, but possibly involves proton pumps or interaction with other membrane proteins, among other possibilities. Since MqsR reduces the production of virtually all proteins including OmpA and OmpF, and simultaneously results in the enrichment of the small transmembrane protein GhoT, it is possible that MqsR increases persistence through a tight control of outer membrane and inner membrane permeability. Another transmembrane peptide TisB has been recently shown to increase persistence by decreasing the proton motive force and ATP levels, thus leading to the formation of dormant cells upon antibiotic stress[7]. Similar to GhoT, production of TisB also leads to cell death by damaging the inner membrane[38]. Collectively, these findings show that certain transmembrane proteins are stress-response elements that are actively involved in persistence.

GhoT resembles the Hok toxin of type I TA pair Hok/Sok from plasmid R1[43, 44]. Five other *hok* homologous loci have been identified in the *E. coli* K-12 genome, *hokA, hokB, hokC, hokD*, and *hokE*. However, all of them appear to be inactivated by various mutations including insertion element transposition or point mutations[45]. Hok utilizes post-segregational killing to stabilize the R1 plasmid[43], but the role of Hok-like toxins as chromosomal loci remains unclear. Also, the link between TA systems and cell death is controversial[10]. Here, we show that GhoT encodes a putative membrane-damaging protein that, in turn, causes persistence at low doses and cell death at high doses. However, it currently is not clear whether the production of GhoT leads to programmed cell death; i.e., perturbing the bacterial membrane by cellular levels of GhoT may be an initial requisite to induce persistence due to loss of membrane potential (cell death is not required and may be an artifact of high level *ghoT* expression).

Although speculative, our results on this novel TA system have several implications for bacterial cell physiology. The first is that the MqsR/MqsA TA system may control persistence through differential mRNA decay via the GhoT/GhoS TA system, which would indicate that TA systems can regulate one another. If *ghoS* mRNA is preferentially cleaved over *ghoT* by MqsR under MqsR/MqsA-inducing conditions, GhoT translated from the enriched *ghoT* RNA would subsequently lead to the formation of ghost cells as well as higher levels of persistence. This delicate control between the two TA systems requires additional detailed investigation. Furthermore, the close relationship between GhoS and the CAS2 CRISPR system suggests that this type of specific RNA cleavage is a general and powerful post-transcriptional approach that has evolved for several purposes in the cell, from controlling cell growth to preventing phage attack. There are suggestions that such systems are global. A report of a similar endoribonuclease VapD from *Helicobacter pylori*[46], also found in a two-gene operon, concluded the RNase was not the toxin of a TA system. However reinterpreting that data in the light of our results suggest the RNase as the antitoxin might be a more parsimonious explanation, suggesting that similar type V TA systems may be found elsewhere. As a result, TA systems are even more complex and diverse in their regulator roles.

EXPERIMENTAL PROCEDURES

Bacterial strains, plasmids, and growth conditions, expression and purification of GhoS for NMR studies, construction of GhoS variants, circular dichroism, purification of His$_6$-GhoS for EMSA assays, the EMSA assays, conditions for the Western blot, NMR spectroscopy, chemical shift assignments and structure calculation, RNA isolation and whole-transcriptome studies, RNA sequencing, mutagenesis of *ghoT* mRNA, and the persister revival assay are described in the Supplementary Methods. Antibiotics, unless specified otherwise, were 50 μg/mL for kanamycin and 30 or 34 μg/mL for chloramphenicol.

Persister cell formation assay

Persister cell measurements were performed as described[6] with slight modifications. To determine the number of persister cells in the presence of MqsR, pCA24N-*mqsR* was introduced into 14 isogenic single gene knockouts (Supplementary Table 2). Overnight cultures of these cells were inoculated into LB medium with chloramphenicol at an initial turbidity at 600 nm of 0.05 and grown for 2.5 h. To induce *mqsR*, 1 mM isopropyl-β-$_D$-thiogalactopyranoside (IPTG) was added for 2 h. Cells were washed with 0.85% NaCl, and the turbidity was adjusted to 1. After exposure to 100 μg/mL ampicillin for 2 h, cells were serially diluted in 0.85% NaCl solution and applied as 10 μL drops to LB plates with chloramphenicol to determine persister cell number[47]. To further evaluate the effect of removing *ghoT* on the formation of persister cells via MqsR, we extended the exposure of 100 μg/mL ampicillin for up to 6 h for BW25113/pCA24N, BW25113/pCA24N-*mqsR*, and ghoT/pCA24N-*mqsR*, and for ghoT/pCA24N-*ghoT* and ghoT/pCA24N. Three independent cultures were used.

Toxicity assay

Overnight cultures of strains producing GhoT via pCA24N-*ghoT*, GhoS via pBS(Kan)-*ghoS*, and variant GhoSX (Y16X) via pBS(Kan)-*ghoSX* were inoculated into 25 mL of LB with kanamycin and chloramphenicol (to maintain both plasmids) to an initial turbidity at 600 nm of of ~ 0.1 with 0.5 mM IPTG, and the turbidity was recorded to determine growth. Three independent cultures were used.

Microscopy

To observe ghost cells, overnight cultures of BW25113/pCA24N-*ghoT*/pBS(Kan) and BW25113/pCA24N-*ghoT*/pBS(Kan)-*ghoS* were diluted to a turbidity of 0.05 at 600 nm and grown to a turbidity of 0.1, and then 0.5 mM IPTG was added to induce *ghoT* and *ghoS*. Cells were collected after 8 h, washed, and resuspended in 0.85% NaCl. Cells were then visualized with light microscopy (Zeiss Axiophot) using an oil immersion objective (63×).

RT-PCR and qRT-PCR

To determine whether *ghoS* and *ghoT* are co-transcribed, reverse transcription-PCR was performed[15]. Total RNA was isolated[4] from BW25113 grown at 37°C during the exponential phase (turbidity was 0.5) with RNA*later*™ (Applied Biosystems). cDNA was synthesized from total RNA with reverse transcriptase (Promega) and random hexamer primers (Invitrogen)[4]. Standard PCR was performed with *Pfu* DNA polymerase using 50 ng of cDNA as template, and using primer pair g*hoS*-f and *ghoT*-r and primer pair *ghoS*-f and *ghoS*-r (Supplementary Table 3). Total RNA and genomic DNA (~50 ng) were also used as templates for the negative and positive controls, respectively.

For qRT-PCR, 50 ng of total RNA was used in each reaction using the *Power* SYBR® Green RNA-to-C_T™ *1-Step* Kit and the StepOne™ Real-Time PCR System (Applied Biosystems). Primers were annealed at 60°C, and *rrsG*[9] expression was used to normalize the data.

Site-directed mutagenesis

Site-directed mutagenesis[9] was used to introduce a stop codon into the coding region of *ghoS* in pBS(Kan)-*ghoS* using primer pair GhoS-X-f/GhoS-X-r (Supplementary Table 3). DNA sequencing using the BigDye Terminator Cycle Sequencing kit was performed to confirm the targeted mutations at these sites.

Crystal violet biofilm assay

Biofilm formation was assayed in 96-well polystyrene plates using 0.1% crystal violet staining[48]. Briefly, overnight cultures of the wild-type, *ghoS* and *ghoT* strains were inoculated at an initial turbidity at 600 nm of 0.05 and grown without shaking for 8 h and 24 h in LB medium. Biofilm formation was normalized by the bacterial growth for each strain (turbidity at 620 nm), and two independent cultures were used for each strain.

Swimming motility assay

Cell motility was examined as described previously on low-salt soft agar plates (1% tryptone, 0.25% NaCl, and 0.3% agar) where the wild-type BW25113 is motile[49].

GhoS RNA cleavage assay

For the synthesis of *ghoS, ghoT, atpE, ompA*, and *ghoT* mRNAs carrying different mutations, PCR products were obtained using the primers shown in Supplementary Table 7 and were used as templates for *in vitro* transcription with T7 RNA polymerase. The T7 RNA polymerase promoter sequence was included in the forward primers. The primers (without the T7 RNA polymerase promoter sequences) for making the *ghoS* and *ghoT* mRNAs are shown in Supplementary Figure 1c (double-underlined). PCR products were gel-purified, and 0.5 to 1 μg of the PCR product was used as the template for the *in vitro* RNA reaction with the AmpliScribe T7-*Flash* transcription kit (Epicentre). The reaction mixture for the GhoS endoribonuclease cleavage assay (10 μL) contained 2 μg RNA, 50 mM Tris-HCl (pH 8.5), 100 mM KCl, 2.5 mM $MgCl_2$, and 30 μg of purified GhoS protein. RNA substrates included *ghoS, ghoT, atpE, ompA, ghoT*m1, *ghoT*m2, *ghoT*m3, *ghoT*m4, and *ghoT*m1m2 mRNAs, total RNAs isolated from BW25113 wild-type cells (OD ~ 2.0), and *E. coli* total tRNAs (Roche). The reaction mixture was incubated at 37°C for 3 h and quenched by the addition of an equal volume of 2X TBE-urea sample buffer (Invitrogen). To inactivate GhoS, protein samples were heated at 95°C for 1 h and were cooled before adding to the reactions. The reaction products were resolved by 15% TBE-urea gels (Invitrogen).

Statistical analysis

Data are presented as means ± s.e. of three or more independent cultures. Statistical significance was assessed using two-tailed unpaired Student's *t*-test.

Supplementary Material

Refer to Web version on PubMed Central for supplementary material.

ACKNOWLEDGEMENTS

REFERENCES

1. Gerdes K, Christensen SK, Lobner-Olesen A. Prokaryotic toxin-antitoxin stress response loci. Nat. Rev. Microbiol. 2005; 3:371–382. [PubMed: 15864262]

2. Hayes F, Van Melderen L. Toxins-antitoxins: diversity, evolution and function. Crit. Rev. Biochem. Mol. Biol. 2011; 46:386–408. [PubMed: 21819231]

3. Masuda H, Tan Q, Awano N, Wu K-P, Inouye M. YeeU enhances the bundling of cytoskeletal polymers of MreB and FtsZ, antagonizing the CbtA (YeeV) toxicity in *Escherichia coli*. Mol. Microbiol. 2012; 84:979–989. [PubMed: 22515815]

4. Ren D, Bedzyk LA, Thomas SM, Ye RW, Wood TK. Gene expression in *Escherichia coli* biofilms. Appl. Microbiol. Biotechnol. 2004; 64:515–524. [PubMed: 14727089]

5. Kim Y, Wang X, Qun M, Zhang X-S, Wood TK. Toxin-antitoxin systems in *Escherichia coli* influence biofilm formation through YjgK (TabA) and fimbriae. J. Bacteriol. 2008; 191:1258–1267. [PubMed: 19060153]

6. Kim Y, Wood TK. Toxins Hha and CspD and small RNA regulator Hfq are involved in persister cell formation through MqsR in *Escherichia coli*. Biochem. Biophys. Res. Commun. 2010; 391:209–213. [PubMed: 19909729]

7. Dörr T, Vuli M, Lewis K. Ciprofloxacin causes persister formation by inducing the TisB toxin in *Escherichia coli*. PLoS Biol. 2010; 8:e1000317. [PubMed: 20186264]

8. Hu Y, Benedik MJ, Wood TK. Antitoxin DinJ influences the general stress response through transcript stabilizer. CspE. Environ. Microbiol. 2012; 14:669–679. [PubMed: 22026739]

9. Wang X, et al. Antitoxin MqsA helps mediate the bacterial general stress response. Nat. Chem. Biol. 2011; 7:359–366. [PubMed: 21516113]

10. Wang X, Wood TK. Toxin/antitoxin systems influence biofilm and persister cell formation and the general stress response. Appl. Environ. Microbiol. 2011; 77:5577–5583. [PubMed: 21685157]

11. Amitai S, Kolodkin-Gal I, Hananya-Meltabashi M, Sacher A, Engelberg-Kulka H. *Escherichia coli* MazF leads to the simultaneous selective synthesis of both "death proteins" and "survival proteins". PLoS Genet. 2009; 5:e1000390. [PubMed: 19282968]

12. Belitsky M, et al. The *Escherichia coli* Extracellular Death Factor EDF induces the endoribonucleolytic activities of the toxins MazF and ChpBK. Mol. cell. 2011; 41:625–635. [PubMed: 21419338]

13. González Barrios AF, et al. Autoinducer 2 controls biofilm formation in *Escherichia coli* through a novel motility quorum-sensing regulator (MqsR, B3022). J. Bacteriol. 2006; 188:305–316. [PubMed: 16352847]

14. Kim Y, et al. *Escherichia coli* toxin/antitoxin pair MqsR/MqsA regulate toxin CspD. Environ. Microbiol. 2010; 12:1105–1121. [PubMed: 20105222]

15. Yamaguchi Y, Park J-H, Inouye M. MqsR, a crucial regulator for quorum sensing and biofilm formation, is a GCU-specific mRNA interferase in *Escherichia coli*. J. Biol. Chem. 2009; 284:28746–28753. [PubMed: 19690171]

16. Christensen-Dalsgaard M, Jørgensen MG, Gerdes K. Three new RelE-homologous mRNA interferases of *Escherichia coli* differentially induced by environmental stresses. Mol. Microbiol. 2010; 75:333–348. [PubMed: 19943910]

17. Domka J, Lee J, Bansal T, Wood TK. Temporal gene-expression in *Escherichia coli* K-12 biofilms. Environ. Microbiol. 2007; 9:332–346. [PubMed: 17222132]

18. Lewis K. Persister cells, dormancy and infectious disease. Nat. Rev. Microbiol. 2007; 5:48–56. [PubMed: 17143318]

19. Lewis K. Persister cells. Annu. Rev. Microbiol. 2010; 64:357–372. [PubMed: 20528688]

20. Brown BL, et al. Three dimensional structure of the MqsR:MqsA complex: A novel TA pair comprised of a toxin homologous to RelE and an antitoxin with unique properties. PLoS Pathog. 2009; 5:e1000706. [PubMed: 20041169]

21. Keren I, Shah D, Spoering A, Kaldalu N, Lewis K. Specialized persister cells and the mechanism of multidrug tolerance in *Escherichia coli*. J. Bacteriol. 2004; 186:8172–8180. [PubMed: 15576765]

22. Correia FF, et al. Kinase activity of overexpressed HipA is required for growth arrest and multidrug tolerance in *Escherichia coli*. J. Bacteriol. 2006; 188:8360–8367. [PubMed: 17041039]

23. Shah D, et al. Persisters: a distinct physiological state of *E. coli*. BMC Microbiol. 2006; 6:53. [PubMed: 16768798]

24. Balaban NQ, Merrin J, Chait R, Kowalik L, Leibler S. Bacterial Persistence as a Phenotypic Switch. Science. 2004; 305:1622–1625. [PubMed: 15308767]

25. Hofmann K, Stoffel W. TMBASE - A database of membrane spanning protein segments. Biol. Chem. 1993; 374:166. Hoppe-Seyler.

26. Faridani OR, Nikravesh A, Pandey DP, Gerdes K, Good L. Competitive inhibition of natural antisense Sok-RNA interactions activates Hok-mediated cell killing in *Escherichia coli*. Nucl. Acids Res. 2006; 34:5915–5922. [PubMed: 17065468]

27. Baba T, et al. Construction of *Escherichia coli* K-12 in-frame, single-gene knockout mutants: the Keio collection. Mol. Syst. Biol. 2006; 2 2006.0008.

28. Van Melderen L, Saavedra De Bast M. Bacterial toxin–antitoxin systems: More than selfish entities? PLoS Genet. 2009; 5:e1000437. [PubMed: 19325885]

29. Guntert P. Automated NMR structure calculation with CYANA. Methods Mol. Biol. 2004; 278:353–378. [PubMed: 15318003]

30. Herrmann T, Guntert P, Wuthrich K. Protein NMR structure determination with automated NOE-identification in the NOESY spectra using the new software ATNOS. J. Biomol. NMR. 2002; 24:171–189. [PubMed: 12522306]

31. Herrmann T, Guntert P, Wuthrich K. Protein NMR structure determination with automated NOE assignment using the new software CANDID and the torsion angle dynamics algorithm DYANA. J. Mol. Biol. 2002; 319:209–227. [PubMed: 12051947]

32. Brunger AT, et al. Crystallography & NMR system: A new software suite for macromolecular structure determination. Acta Crystallogr. D Biol. Crystallogr. 1998; 54:905–921. [PubMed: 9757107]

33. Holm L, Kaariainen S, Rosenstrom P, Schenkel A. Searching protein structure databases with DaliLite v.3. Bioinformatics. 2008; 24:2780–2781. [PubMed: 18818215]

34. Orengo CA, Jones DT, Thornton JM. Protein superfamilies and domain superfolds. Nature. 1994; 372:631–634. [PubMed: 7990952]

35. Beloglazova N, et al. A novel family of sequence-specific endoribonucleases associated with the clustered regularly interspaced short palindromic repeats. J. Biol. Chem. 2008; 283:20361–20371. [PubMed: 18482976]

36. Samai P, Smith P, Shuman S. Structure of a CRISPR-associated protein Cas2 from Desulfovibrio vulgaris. Acta Crystallogr. Sect. F Struct. Biol. Cryst. Commun. 2010; 66:1552–1556.

37. Beloglazova N, et al. A novel family of sequence-specific endoribonucleases associated with the clustered regularly interspaced short palindromic repeats. J. Biol. Chem. 2008; 283:20361–20371. [PubMed: 18482976]

38. Unoson C, Wagner EGA. A small SOS-induced toxin is targeted against the inner membrane in *Escherichia coli*. Mol. Microbiol. 2008; 70:258–270. [PubMed: 18761622]

39. de la Hoz AB, et al. Plasmid copy-number control and better-than-random segregation genes of pSM19035 share a common regulator. Proc. Natl. Acad. Sci. USA. 2000; 97:728–733. [PubMed: 10639147]

40. Donegan NP, Cheung AL. Regulation of the *mazEF* toxin-antitoxin module in *Staphylococcus aureus* and its impact on *sigB*expression. J. Bacteriol. 2009; 191:2795–2805. [PubMed: 19181798]

41. Jayaraman R. Bacterial persistence: some new insights into an old phenomenon. J. Biosci. 2008; 33:795–805. [PubMed: 19179767]

42. Maisonneuve E, Shakespeare LJ, Jørgensen MG, Gerdes K. Bacterial persistence by RNA endonucleases. Proc. Natl. Acad. Sci. USA. 2011; 108:13206–13211. [PubMed: 21788497]

43. Gerdes K. The *parB* (*hok/sok*) locus of plasmid R1: A general purpose plasmid stabilization system. Nat. Biotechnol. 1988; 6:1402–1405.

44. Pecota DC, Wood TK. Exclusion of T4 phage by the *hok/sok* killer locus from plasmid R1. J. Bacteriol. 1996; 178:2044–2050. [PubMed: 8606182]

45. Pedersen K, Gerdes K. Multiple *hok* genes on the chromosome of *Escherichia coli*. Mol. Microbiol. 1999; 32:1090–1102. [PubMed: 10361310]

46. Kwon A-R, et al. Structural and biochemical characterization of HP0315 from *Helicobacter pylori* as a VapD protein with an endoribonuclease activity. Nucleic Acids Res. 2012 published online 12 January.

47. Donegan K, Matyac C, Seidler R, Porteous A. Evaluation of methods for sampling, recovery, and enumeration of bacteria applied to the phylloplane. Appl. Environ. Microbiol. 1991; 57:51–56. [PubMed: 16348404]

48. Fletcher M. The effects of culture concentration and age, time, and temperature on bacterial attachment to polystyrene. Can. J. Microbiol. 1977; 23:1–6.

49. González Barrios AF, Zuo R, Ren D, Wood TK. Hha, YbaJ, and OmpA regulate *Escherichia coli* K12 biofilm formation and conjugation plasmids abolish motility. Biotechnol. Bioeng. 2006; 93:188–200. [PubMed: 16317765]
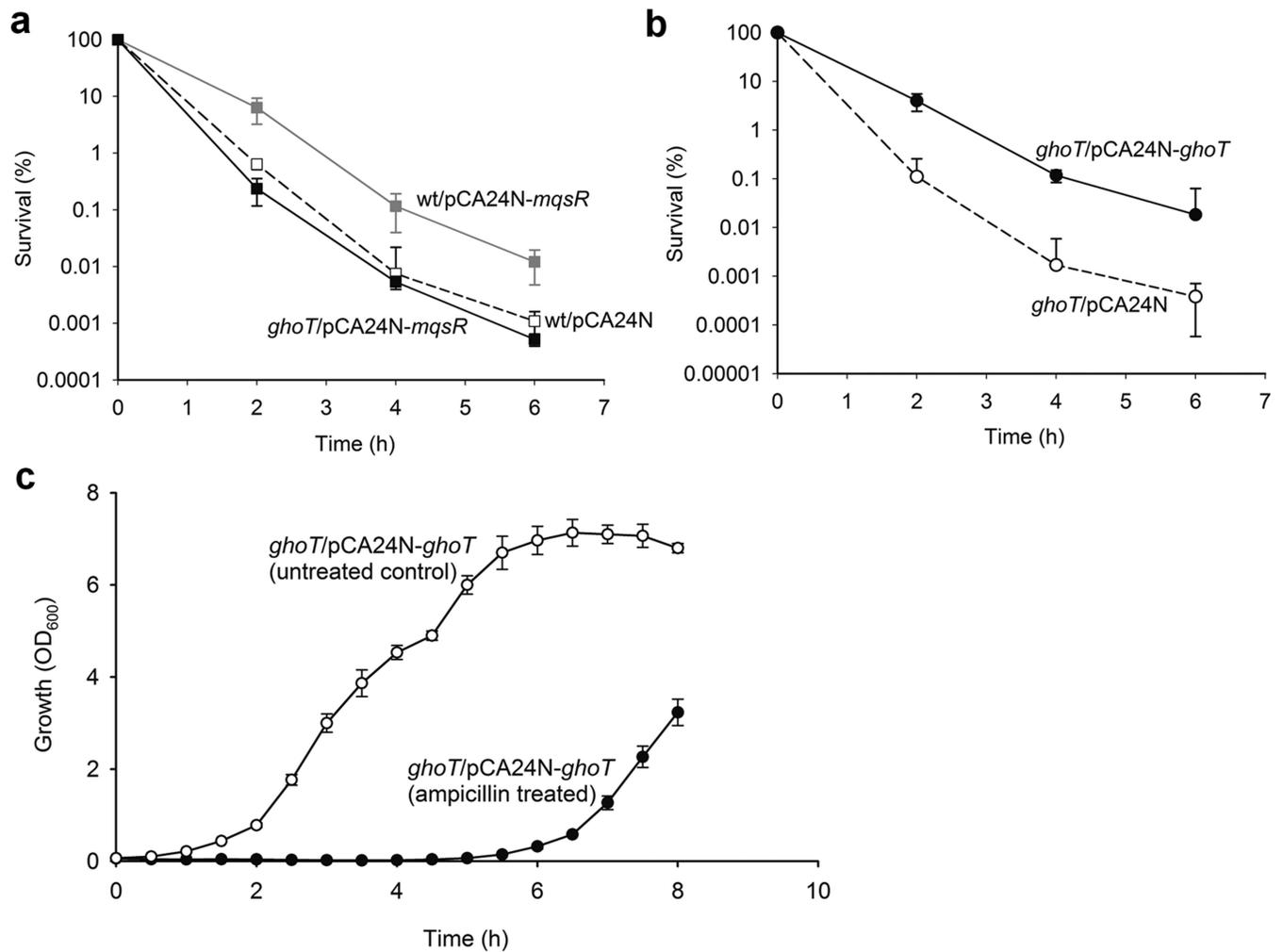
Fig. 1. GhoT increases persistence

Cell survival (%) after ampicillin (100 μg/mL) treatment for 2, 4, and 6 h with MqsR production with and without *ghoT* (**a**), or with GhoT production (**b**). wt indicates the wild-type host (*E. coli* BW25113). (**c**) Revival of GhoT-induced persister cells was tested by producing GhoT in BW25113 *ghoT*/pCA24N-*ghoT* while treating cells with ampicillin (100 μg/ml) for 2 hours. Growth in fresh LB medium was compared to control cells that lacked ampicillin treatment. At least three independent cultures of each strain were evaluated for each experiment, and error bars indicate standard error of mean.
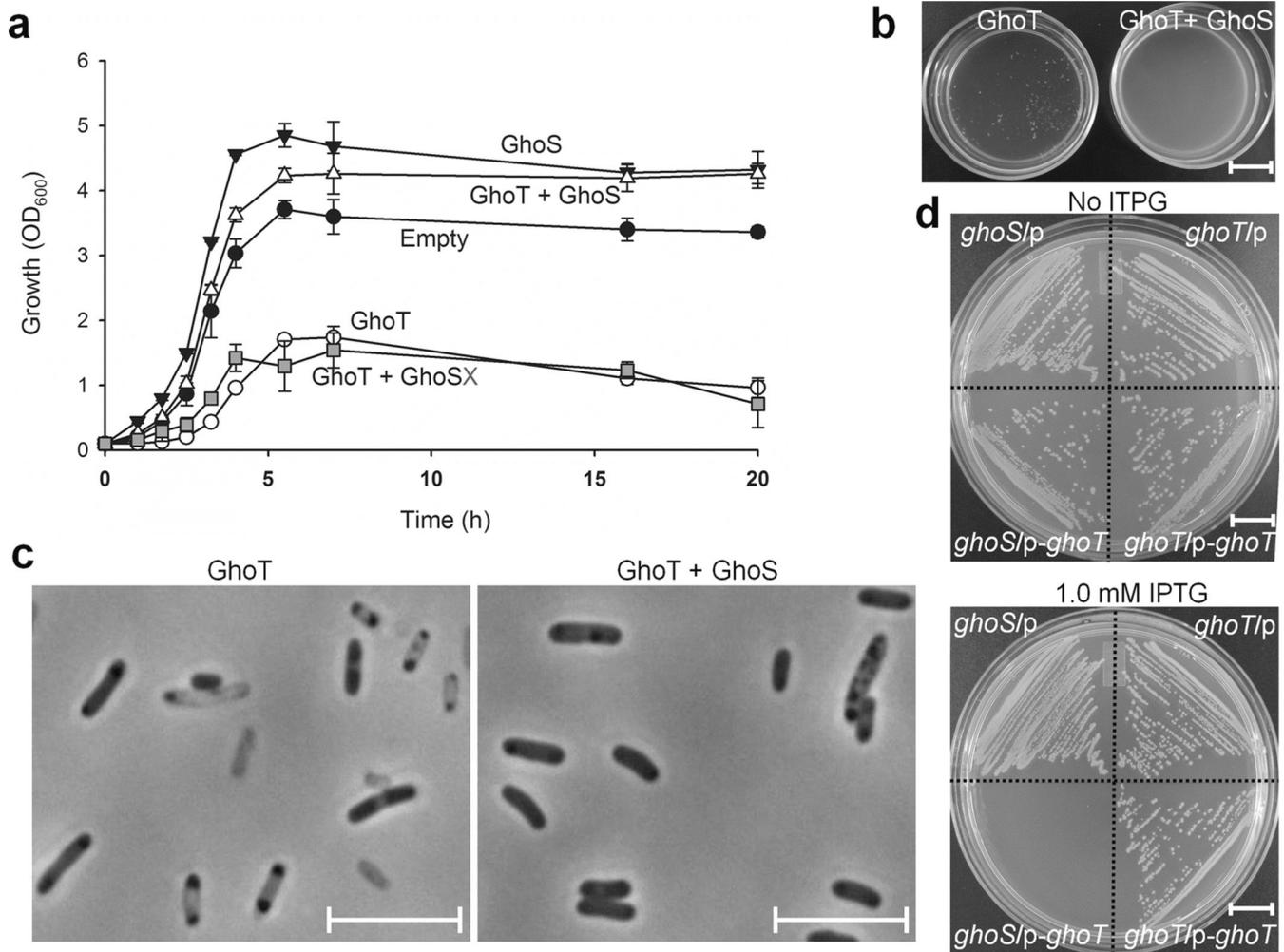
Fig. 2. GhoT is toxic and GhoS reduces this toxicity
(a) Cell growth in LB medium for cells producing GhoT and GhoS. Note the chromosomal copy of *ghoS* in the wild-type strain allows for some growth with toxin GhoT production. GhoSX is truncated GhoS with a stop codon introduced at Tyr16. Three independent cultures of each strain were evaluated, and error bars indicate standard error of mean ($n = 3$). **(b)** Cell culture at the end of growth in (**a**) at 20 h to show the clearance and lysis due to production of GhoT. Scale bar represents 1 cm. **(c)** Cell morphology after incubating for 8 h at 37°C. Scale bar represents 5 μm. For (**a**), (**b**) and (**c**), Empty: BW25113/pCA24N/pBS(Kan), GhoT: BW25113/pCA24N-*ghoT*/pBS(Kan), GhoS: BW25113/pCA24N/pBS(Kan)-*ghoS*, GhoT + GhoS: BW25113/pCA24N-*ghoT*/pBS(Kan)-*ghoS*, and GhoT + GhoSX: BW25113/pCA24N-*ghoT*/pBS(Kan)-*ghoSX*. Plasmids were retained with kanamycin (50 μg/mL) and chloramphenicol (30 μg/mL); 0.5 mM IPTG was used at time 0 to produce the plasmid-based proteins. Three independent cultures of each strain were evaluated. **(d)** Growth on LB plates with kanamycin (50 μg/mL), chloramphenicol (30 μg/mL), and IPTG (1 mM, to induce *ghoT* via pCA24N-*ghoT*). In the absence of a chromosomal copy of *ghoS*, there is no growth with toxin GhoT production. Δ*ghoS* is BW25113 Δ*ghoS* and Δ*ghoT* is BW25113 Δ*ghoT*. p refers to pCA24N and p-*ghoT* refers to

pCA24N-*ghoT*, respectively. Three independent cultures of each strain were evaluated. Scale bar represents 1 cm.
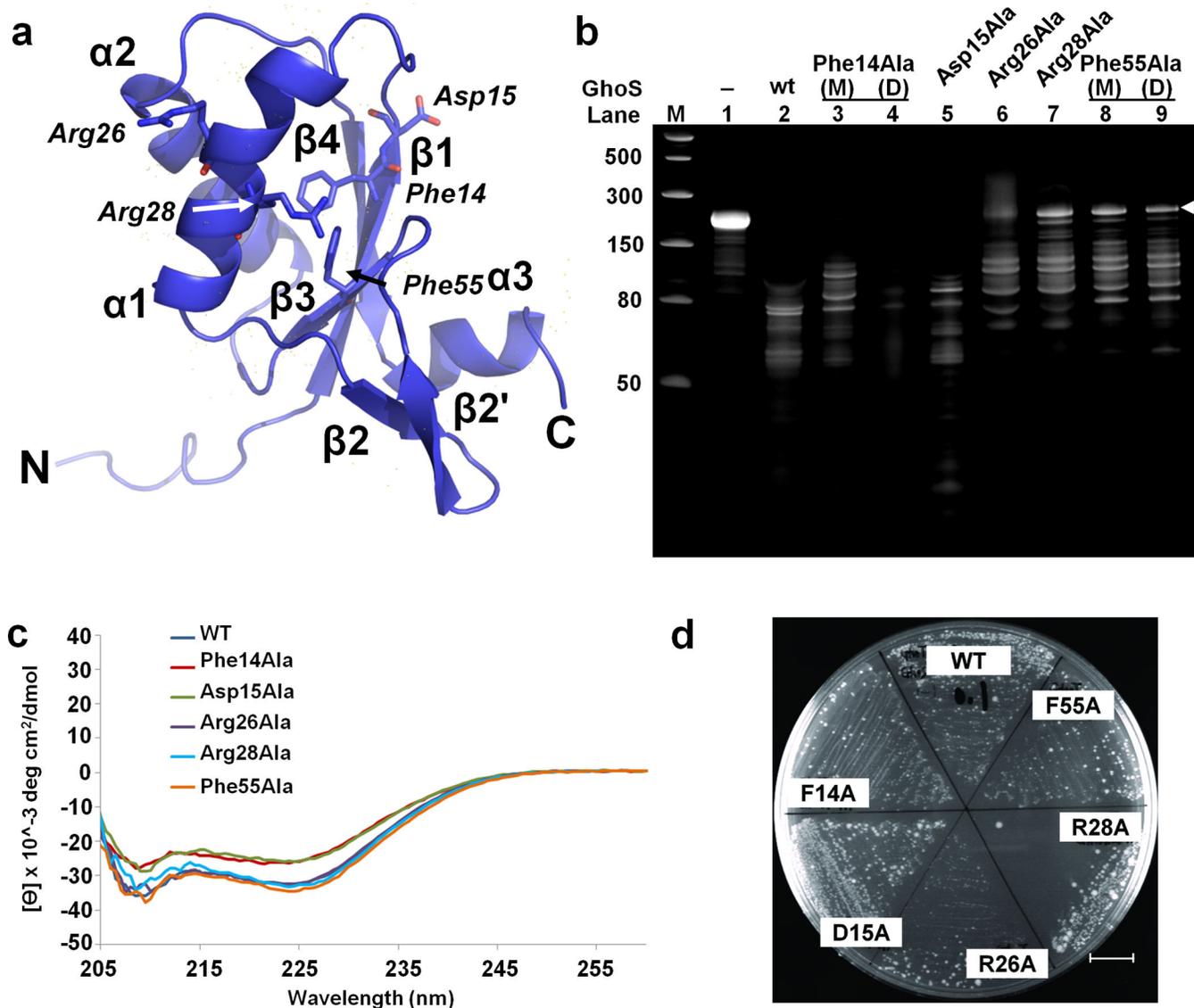
Fig. 3. GhoS adopts a ferredoxin-like fold and Arg28 is important for its cleavage activity
(a) Ribbon model of the lowest-energy conformer of GhoS, with the secondary structural elements and termini labeled; putative catalytically important residues shown as sticks and labeled. Figure prepared with PyMOL (http://www.pymol.org/). **(b)** Two-micrograms of *in vitro* synthesized wild-type *ghoT* transcript (207 nt, lane 1) were incubated without (−) or with 30 μg of purified GhoS and its variants at 37°C for 3 h. Two mutants, F14A and F55A, eluted from the size exclusion column as monomers (M) and dimers (D), so both forms were tested (F14A, 40% dimer; F55A, 32% dimer). The reduced activity of GhoS with point mutations is shown by the presence of un-cleaved transcript as indicated by an arrow. M indicates low range ssRNA ladder. **(c)** Circular dichroism (CD) spectra demonstrating that native GhoS (dark blue) and all the GhoS mutants are folded (sample concentrations ~20 μM). **(d)** Co-expression of GhoT with wild-type (WT) GhoS and the GhoS variants via BL21(DE3)/pCA24N-*ghoT* harboring the pRP1B(Kan)-*ghoS* constructs (0.1 mM IPTG was used). Scale bar represents 1.1 cm.
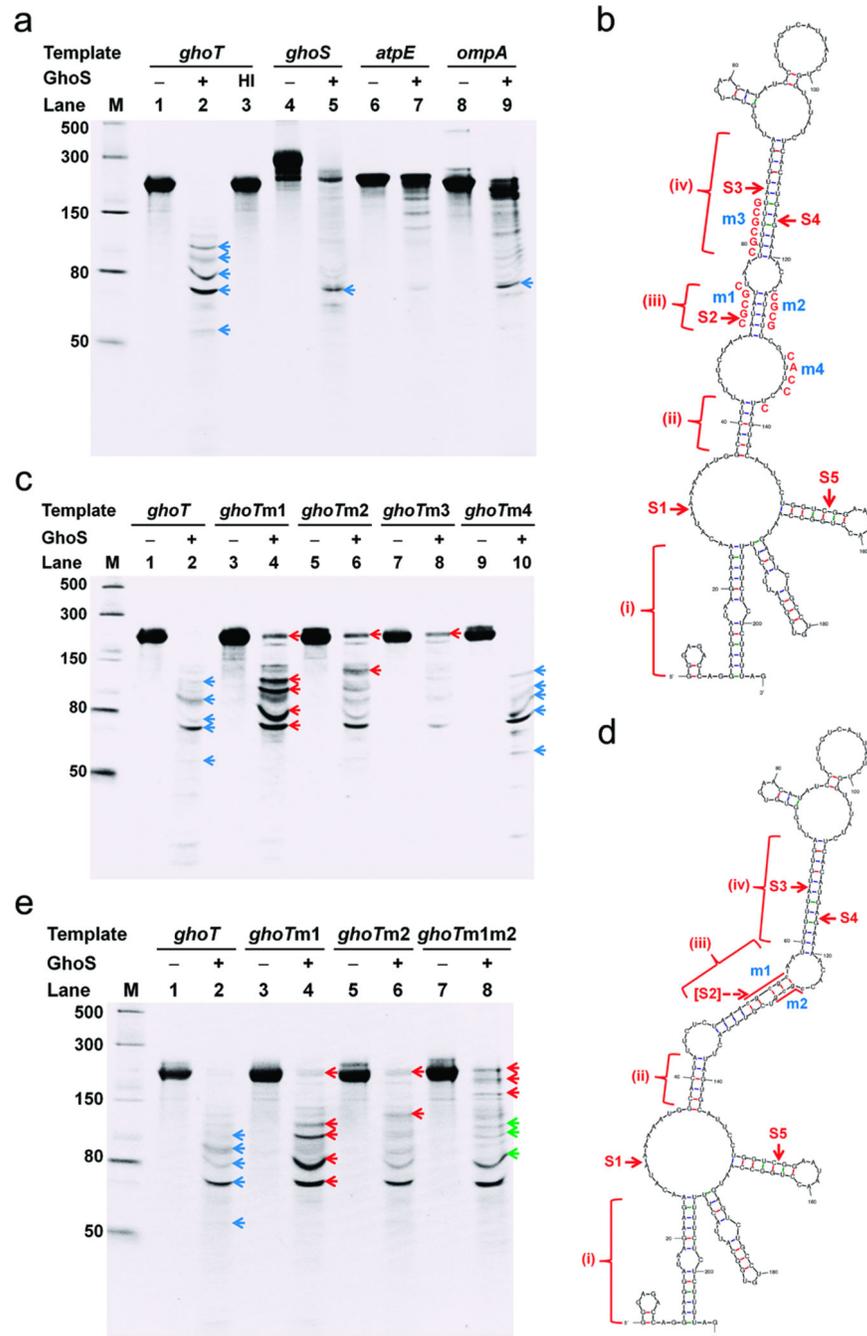
Fig. 4. GhoS cleavage of native and altered *ghoT* transcripts

(**a**) GhoS cleavage reaction with native transcripts of *ghoT* (207 nt), *ghoS* (311 nt), *atpE* (189 nt) and *ompA* (211 nt). HI indicates heat inactivated GhoS. The blue arrows indicate the main fragments generated after cleavage. M indicates the low range ssRNA ladder. **(b)** Predicted secondary structure of *in vitro* synthesized *ghoT* mRNA. Capital red letters indicate the changed nt for mutations m1, m2, m3, and m4. S1, S2, S3, S4, and S5 indicate the cleavage sites based on RNA sequencing. The four main sections in the structure are indicated with numbers i, ii, iii and iv. The RNA secondary structure was obtained using

Mfold software. (**c**) GhoS cleavage reaction with transcripts of *ghoT* with mutations m1, m2, m3, and m4 (207 nt). The red arrows indicate the fragments generated or increased in the mutant transcripts after cleavage. (**d**) Predicted secondary structure of *in vitro* synthesized *ghoT*m1m2 mRNA. The mutated *ghoT*m1m2 cleavage site is indicated by two solid red lines. (**e**) GhoS cleavage reaction with transcripts of *ghoT* with mutations m1, m2, and m1m2 (207 nt). The green arrows indicate the reduced fragments after the introduction of the second mutation. For the reactions shown in (**a**), (**c**), and (**e**), 2 μg of *in vitro* synthesized transcripts were incubated in with (−) or without 30 μg (+) of purified GhoS at 37°C for 3 h and analyzed by gel electrophoresis.